NASA-TM-104184 19920009635

**NASA Technical Memorandum 104184**

# Thermal / Structural Analysis of a Transpiration Cooled Nozzle

**Peyton B. Gregory**
**Jon E. Thompson**
**Dale A. Babcock**
**Carl E. Gray Jr.**
**Chris A. Mouring**



**February 1992**

NASA
National Aeronautics and Space Administration
**Langley Research Center**
Hampton, Virginia 23665-5225

# Table of Contents

## Appendix II Mass Flow Model



## Appendix III Platelet Flutter Analysis

# List of Figures



# List of Tables

# List of Symbols

$c_0$ = orifice coefficient

$c_1$ = recovery coefficient

$c_g$ = flow coefficient

$c_v$ = constant volume specific heat coefficient

$c_p$ = constant pressure specific heat coefficient

g = gravity constant

h = heat transfer coefficient

$h_{4000}$ = heat transfer coefficient at 4000 psi combustor pressure

$\dot{m}$ = mass flow

$\dot{m}_{in}$ = mass flow in

$\dot{m}_{out}$ = mass flow out

n = polytropic exponent

p = pressure

$p_f$ = final pressure

$p_i$ = initial pressure

v = volume

A = area

C = constant

$\dot{E}$ = volume energy derivative

L = length

M = volumetric mass

$\dot{M}$ = volume mass derivative

Nu = Nusselt number

$\dot{P}$ = volume pressure derivative

$P_{down}$ = pressure downstream

$P_{up}$ = pressure upstream

Pr = Prandtl number

R = real gas constant

Re = Reynolds number

$Re_{4000}$ = Reynolds number at 4000 psi combustor pressure

$T$ = temperature

$\dot{T}$ = volume temperature derivative

$T_f$ = final temperature

$T_i$ = initial temperature

$T_{in}$ = temperature in

$T_{out}$ = temperature out

$Z$ = compressibility factor

$\Delta L_{bulk}$ = change in length between room temperature and bulk temperature

$\Delta L_{ID}$ = change in length between room temperature and the maximum expansion at the inner diameter from the local FEM's of the stacks

$\Delta P$ = change in pressure

$\Delta T$ = change in temperature

$\Delta T_{bulk}$ = bulk temperature difference between the platelet stacks and the housings under the 4000. psi Hot-Min case

$\mu$ = viscosity

$\mu_{4000}$ = viscosity at 4000 psi combustor pressure

$v$ = specific volume

# 1.0 Introduction

The 8-foot High Temperature Tunnel (HTT) at NASA Langley Research Center is a combustion driven, high enthalpy blow down wind tunnel. The 8 foot diameter by 12 foot long free jet test section is designed to achieve Mach 4, 5, and 7 with true temperature simulation. The combustor which burns methane and air or methane, air, and LOX, is composed of three main components; the barrel, the quick actuating closure plug, and the transpiration cooled nozzle.

In March 1991, during check out of the transpiration cooled nozzle, pieces of platelets were found in the tunnel test section. It was determined that the pieces came from the throat region of the nozzle. Further investigation discovered that there were gaps at various locations between the platelet stacks. The decision was made to take the nozzle apart to determine the cause of the failed platelets and gaps between the platelet stacks. The results indicated there were three main factors which attributed to the failure of the platelets; first was the fact that there were unbonded platelets between the bonded stacks (only the loose platelets failed), secondly was the tolerancing associated with the platelet stacks and housing tang at station -2.75 (see Fig. 1) which resulted in gaps between the platelet stacks i.e. platelets were not in compression, and thirdly, was the corrosive environment in which the loose platelets were subjected to and magnified by the fact that the loose platelets were full hard and more subject to corrosion. In summary, the loose platelets corroded and since the platelets were not in compression they were easily blown out by the manifold air.

A platelet flutter analysis was performed in Appendix III to evaluate the loose platelets. The loose platelet factor was resolved by 'copper assisted diffusion bonding' all sets of unbonded platelets. This resulted in a set of mini-stacks which were oversized and then machined to attain an appropriate tolerance level.

The objective of this analysis is to determine the tolerance layout between the platelets and the housing to meet the structural and performance criteria under a range of thermal, pressure, and bolt preload conditions. In addition, bolt preloads and an assembly procedure will be specified. To accomplish this, a detailed thermal / structural finite element analysis of the combustor nozzle, pressure shell, and end closure plug was performed using EAL (Ref. 1) analysis software and PATRAN (Ref. 2) model development. Additional models were developed of several platelet stacks to incorporate the local effects of stack heating.

# 2.0 Component Description

The transpiration cooled nozzle shown in Figure 1 consists of four housings (which are defined by a three digit number) and 15 platelet stacks. Platelet stack 11 was incorporated into stack 10 and is therefore not shown. There are eight circuits which are supplied independent mass flows to attain a maximum surface temperature along the nozzle contour of $900^0$F. The upstream contraction section has an inner diameter of 36.0 inches, the throat has an inner diameter of 5.6 inches, and the exit has an inner diameter of 18.6 inches. The nozzle is 84.9 inches long and is secured to the pressure shell by 12 keyed segments bolted

to the housing. The platelet stacks consist of a series of paired platelets which are diffusion bonded together. A pair of platelets consists of a metering and an etched platelet. Before diffusion bonding, the platelets are lined up to achieve the proper mass flows and pressure drops required by that particular section. Table 1 gives the material properties of the nozzle components.

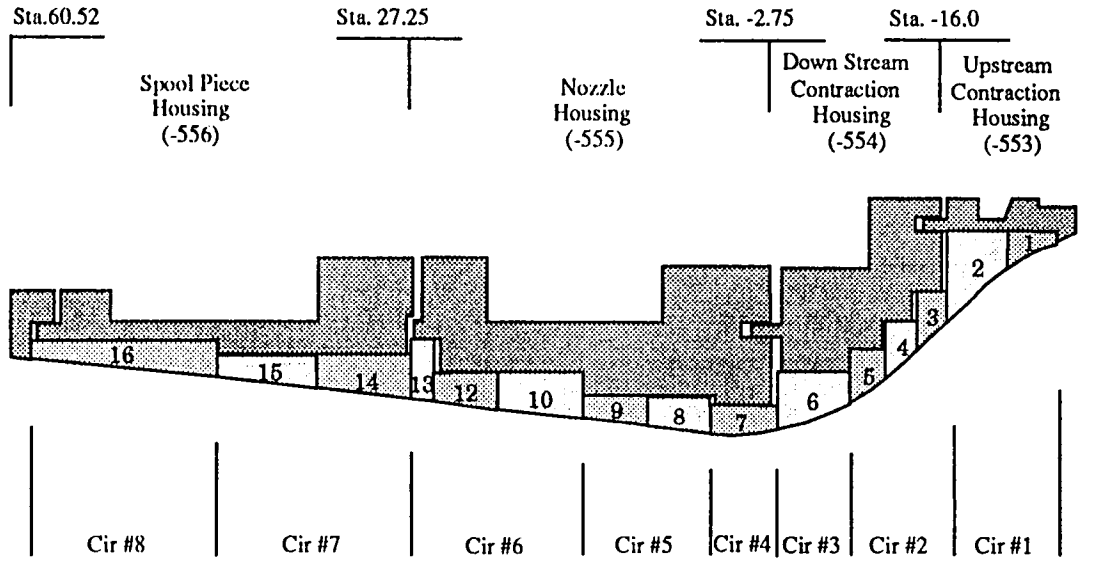


**Figure 1. Transpiration Cooled Nozzle Layout.**

**Table 1. Material Properties.**

| Component | Material | Tensile Strength (ksi) | Yield Strength (ksi) |
|---|---|---|---|
| Pressure Housing | SA-336(304L) | 65.0 | 25.0 |
| Loose Platelets | 347 SS(full hard) | 185.0 | 150.0 |
| Bonded platelets | 347 SS | 70.0 | 30.0 |
| Bolts | SA-354 Gr BD | 150.0 | 130.0 |

## 3.0 Criteria

The nozzle criteria include both structural and performance criteria. The structural criteria is applied to maintain the integrity and safety in terms of pressure vessel design. There are normal operating loads and emergency loads. Under normal loads, a standard pressure vessel design code is used. Under emergency conditions a criteria is used to prevent permanent distortion. The initial design met the structural criteria under all pressure load cases. The main consideration in this analysis is the addition of thermal loads as applied to the platelets, pressure housings, and bolts. The performance criteria is applied to ensure that the nozzle meets cooling and flow requirements. The general requirement is to insure that platelet stacks or circuits are not starved of air by gapping

between stacks or circuits. The performance requirements are only considered under hot run conditions. The structural and performance criteria is defined below.

- Structural Criteria
  - Normal Operating: ASME Boiler & Pressure Vessel Code, Section VIII, Div. I
  - Emergency Condition: Maximum Stress < .9(Yield Stress)
- Performance Criteria
  - Platelet stacks should remain in compression (load > 0) for hot run conditions.
  - Maximun bypass between circuits should be 5% or less for hot run conditions.

# 4.0 Load Matrix

The loadings are based on three factors; combustor pressure, combustor temperature, and the amount of cooling mass flow applied to the eight circuits supplying the nozzle. Three combustor pressures were considered; 4000 psi, 2000 psi, and 700 psi. In addition an emergency valve open case was considered under cold flow conditions. The combustor temperature used for all hot cases was $3669^0$F. Two conditions were considered for each combustor pressure in terms of circuit cooling; a 'Hot-Min' case in which the circuits are 20% over cooled, and a 'Hot-Max' case in which the circuits are 20% under cooled. This was considered to determine the effects of under or over cooling the circuits. To determine the maximum possible gapping between the platelet stacks, a cold flow case was considered for the three combustor pressures. Table 2 is a summary of the load cases considered in this analysis.

**Table 2. Load Cases.**

| Case | Combustor Pressure, psi | Nozzle Temperature |
|---|---|---|
| 1 | 4000 | Hot-Min |
| 2 | 4000 | Hot-Max |
| 3 | 4000 | Cold |
| 4 | 2000 | Hot-Min |
| 5 | 2000 | Hot-Max |
| 6 | 2000 | Cold |
| 7 | 700 | Hot-Min |
| 8 | 700 | Hot-Max |
| 9 | 700 | Cold |
| 10 | Emerg. Valve Open | Cold |

## 4.1 Pressure Loads

Table 3 is a summary of the pressure loadings as applied to the eight circuits (refer to Fig. 1). The manifold pressure and the nozzle contour pressures are shown for the three

combustor conditions and the emergency valve open case. The manifold pressure is the pressure supplied to the circuit acting on the outer diameter of the platelets and the inner diameter of the housings. The nozzle contour pressure is the pressure acting on the inner diameter of the platelets. At an intersection between two circuits, the maximum manifold pressure of the two is used between the platelet stacks in the analysis.

**Table 3. Pressure Loads, psi.**

| | | Circuit No. | | | | | | | |
|---|---|---|---|---|---|---|---|---|---|
| Comb. Pressure | | 1 | 2 | 3 | 4 | 5 | 6 | 7 | 8 |
| 4000 psi | Manifold | 4330 | 4400 | 4200 | 3900 | 3900 | 1200 | 900 | 600 |
| 4000 psi | Nozzle | 4000 | 4000 | 3740 | 1900 | 1900 | 320 | 100 | 30 |
| 2000 psi | Manifold | 2165 | 2165 | 2165 | 1899 | 1821 | 570 | 384 | 280 |
| 2000 psi | Nozzle | 2000 | 2000 | 1870 | 950 | 950 | 160 | 50 | 15 |
| 700 psi | Manifold | 779 | 769 | 756 | 639 | 513 | 152 | 106 | 106 |
| 700 psi | Nozzle | 700 | 700 | 655 | 332 | 332 | 56 | 18 | 5 |
| Emer. Valve Open | Manifold | 1500 | 1500 | 1500 | 1500 | 5110 | 1573 | 1180 | 787 |
| Emer. Valve Open | Nozzle | 0 | 0 | 0 | 0 | 0 | 0 | 0 | 0 |

## 4.2 Platelet Bulk Temperatures

Table 4 gives the platelet stack bulk temperature differences for the 'Hot-Min', 'Hot-Max', and cold flow conditions under the three combustor pressures.

**Table 4. Platelet Bulk Temperatures Differences, $^{0}$R.**

| Combustor Pressure, 4000 psi | | | | | | | | | | | | | | | |
|---|---|---|---|---|---|---|---|---|---|---|---|---|---|---|---|
| Stack # | 1 | 2 | 3 | 4 | 5 | 6 | 7 | 8 | 9 | 10 | 12 | 13 | 14 | 15 | 16 |
| Hot-Max | 135 | 15 | 10 | 10 | 10 | -5 | -25 | -50 | -55 | -60 | -50 | -45 | -40 | -45 | 25 |
| Hot-Min | 50 | -5 | -10 | -10 | -10 | -15 | -40 | -70 | -75 | -80 | -70 | -55 | -60 | -65 | -20 |
| Cold | -30 | -30 | -30 | -30 | -30 | -35 | -50 | -80 | -90 | -100 | -100 | -100 | -105 | -105 | -110 |

| Combustor Pressure, 2000 psi | | | | | | | | | | | | | | | |
|---|---|---|---|---|---|---|---|---|---|---|---|---|---|---|---|
| Stack # | 1 | 2 | 3 | 4 | 5 | 6 | 7 | 8 | 9 | 10 | 12 | 13 | 14 | 15 | 16 |
| Hot-Max | 225 | 40 | 10 | 5 | 5 | -25 | -40 | -50 | -60 | -60 | -45 | -30 | -40 | 10 | 80 |
| Hot-Min | 90 | -10 | -20 | -30 | -30 | -40 | -50 | -70 | -80 | -80 | -70 | -60 | -70 | -40 | -5 |
| Cold | -50 | -50 | -50 | -50 | -50 | -55 | -65 | -80 | -100 | -105 | -110 | -110 | -110 | -110 | -110 |

| Combustor Pressure, 700 psi | | | | | | | | | | | | | | | |
|---|---|---|---|---|---|---|---|---|---|---|---|---|---|---|---|
| Stack # | 1 | 2 | 3 | 4 | 5 | 6 | 7 | 8 | 9 | 10 | 12 | 13 | 14 | 15 | 16 |
| Hot-Max | 250 | 95 | 50 | -20 | -10 | -40 | -50 | -55 | -55 | -55 | -30 | -15 | -5 | 100 | 220 |
| Hot-Min | 130 | 5 | -15 | -50 | -40 | -65 | -80 | -85 | -85 | -85 | -60 | -45 | -50 | 10 | 95 |
| Cold | -80 | -80 | -80 | -80 | -80 | -85 | -90 | -95 | -100 | -110 | -110 | -110 | -110 | -110 | -110 |

Bulk temperature is the average temperature difference between the platelets and the housings in terms of a global analysis of how the platelet stacks respond to thermal loads. The detailed analysis to determine bulk temperatures of the platelet stacks is given in Appendix I.

## 5.0 Finite Element Model of Nozzle

Figure 2 is a plot of the finite element model in the area of the nozzle. The full model includes the entire combustor shell and the components of the closure plug which enables all the pressure loads to be transmitted through the nozzle. The model is a one degree wedge with axi-symmetric boundary conditions. There are non-linear contact elements at the interface between each section identified by shades of gray. The model is constrained in the axial direction at Station 60.52. To simulate the tolerance level between the housings and the platelets, the interfaces at the housing flanges are allowed to collapse into each other. The bolts are modeled as axial rod elements at Stations 27.25, -2.75, -16.0, and the bolts connecting the keyed section to the nozzle. The bolt preloads are simulated by applying an appropriate negative temperature differential to the rod elements.

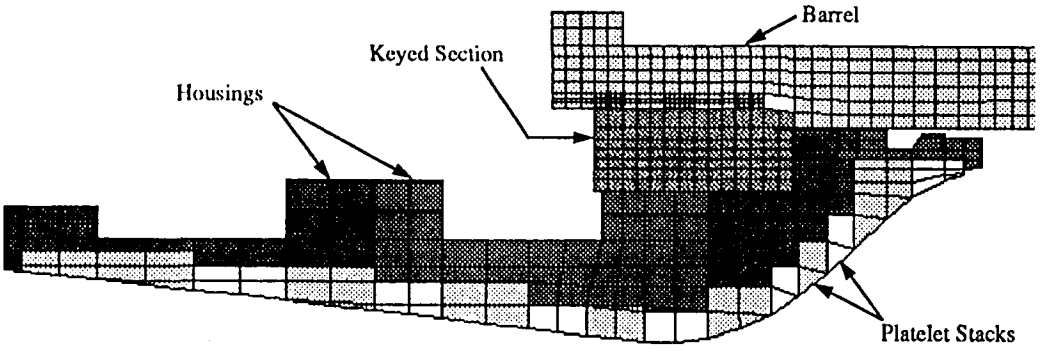


**Figure 2. Finite Element Model of Nozzle.**

## 6.0 Bulk Temperature Analysis

The bulk temperature analysis looks at the global effects of the temperature differential between the platelets and the housings. Under all hot-run conditions the majority of the platelet stacks cool down and tend to contract. To maintain compression under these conditions, the platelets need to be initially oversized and under high compressive forces so that when the platelets contract the compressive forces are reduced but not eliminated. To determined the amount the platelets need to be oversized, the Hot-Min cases were run for the three combustor cases and the flange gaps (the amount the platelets are oversized at the flanges) were adjusted until the platelets remained in compression. It was also considered critical to keep circuits 5 and 6 from communicating due to the high pressure drop across these circuits, see Table 3. Therefore during the iteration, the flange gap at Station 27.25 was increased to maintain contact between stack 10 and the pressure housing. The loads considered were platelet stack bulk temperatures, pressure, and bolt preload. The bolt preloads were adjusted as required to ensure that the flanges remained in contact.

## 6.1 Results

Table 5 shows the results from iterating on the flange gaps to maintain platelet compression and to ensure stack 10 and the housing remain in contact for the Hot-Min condition under the three combustor pressures.

**Table 5. Flange Gaps for the Three Combustor Pressures.**

| Combustor Pressure | Flange Gaps, inches Sta. 27.25 | Sta. -2.75 | |
|---|---|---|---|
| 4000 psi | .026 | .018 | <----- CONTROLS |
| 2000 psi | .020 | .017 | |
| 700 psi | .014 | .012 | |

The 4000 psi case controls, meaning that if the platelet stacks are oversized .026 inches at Station 27.25 and .018 inches at Station -2.75, then the platelets will remain in compression and the clearance between circuits 5 and 6 will be minimal for all combustor pressures. Therefore the hot cases, see Table 2, and the preload case will be analyzed using the flange gaps under the 4000 psi case. Table 6 shows the general results of the analysis in terms of how the components compare to the criteria. The three components considered were the shell, bolts, and the platelets.

**Table 6. Results for .026/.018 Flange Gaps.**

| Pressure | Temperature | Shell | Bolts | Platelets |
|---|---|---|---|---|
| 4000 psi | Hot-Max | OK | OK | OK |
| | Hot-Min | OK | OK | OK |
| 2000 psi | Hot-Max | High | High | OK |
| | Hot-Min | OK | OK | OK |
| 700 psi | Hot-Max | NG | NG | NG |
| | Hot-Min | OK | OK | OK |
| Preload | | OK | OK | High |

In Table 6, 'OK' means the component meets the criteria, 'High' means the component is in a gray area in terms of meeting the criteria and is not desirable, and 'NG' means the component does not meet the criteria. For the hot cases, the problem area is under the Hot-Max case for the 2000 psi and the 700 psi combustor pressures. The major driver towards increasing the stresses is the fact that the platelets in circuits 1 and 8 attain a high bulk temperature under the Hot-Max cases (circuits 20% under cooled), see Table 4. Therefore to meet the criteria at least circuits 1 and 8 need to be 20% over cooled. This eliminates the Hot-Max cases from consideration and leaves only the Hot-Min cases to evaluate which meet the criteria.

For the preload case the platelet stresses are high due to the large compressive loads needed to bring the flanges together. Figure 3 shows a deformed stress contour plot under the preload condition.

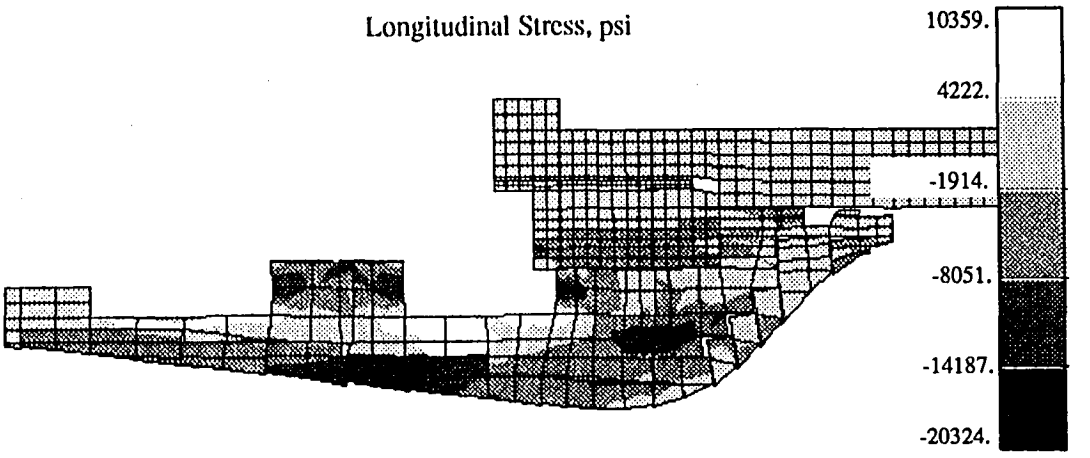


**Figure 3. Stress / Deformation Plot under Preload w/gaps = .026/.018**

The high stresses are located in stacks 10,12 and 13, particularly in stack 12. The stress is below yield stress but is considered high for the platelets due to its porous condition in that excessive loads will tend to close up the flow passages. To lower the stresses, the flange gaps need to be reduced in order to lower the initial preload in the platelets. To accomplish this, more refined thermal models were developed to define the local effects of stack heating.

## 7.0 Local Effects of Stack Heating

The initial results were based on bulk temperatures but under actual conditions the temperature varies through the radial thickness. The variance is such that the inner diameter is hotter than the bulk temperature and the outer diameter is cooler than the bulk temperature. Since the inner diameter gets hotter than the bulk temperature, it expands more and would therefore keep the platelets in compression at the inner diameter using smaller flange gaps. Figure 4 shows an example of three different states that a typical platelet stack can assume.

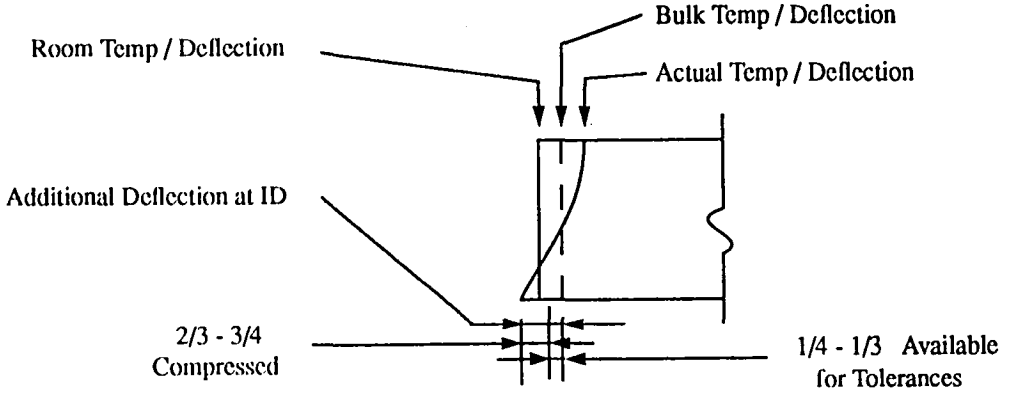


**Figure 4. Local Effects of Stack Heating.**

## 7.1 Local Tolerancing Criteria

Figure 4 shows three platelet stack configurations; room temperature, bulk temperature, and the actual temperature. To take advantage of the actual deflection, the additional deflection (see Figure 4) between the bulk and the actual at the inner diameter was considered. The criteria will be to let 2/3 to 3/4 of the additional deflection attain a compressed state which in turn leaves 1/4 to 1/3 of the additional deflection available for tolerances. This is graphically shown in Figure 4. The additional deflection available for tolerancing will then be used to reduce the flange gaps while maintaining compression in the platelets and reducing the preload stresses in the platelets. To determine the additional deflection, several local finite element models of the platelet stacks were developed using actual thermal gradients through the thickness.

## 7.2 Finite Element Model of Stacks

Finite element models of platelet stacks 6, 7, 8, 10, 14, and 16 were developed to get a good representative sampling of the thermal response of the various stacks (1-16). The stacks which were not modeled, were assumed to act as an adjacent stack which was modeled. The models have a course element mesh where the thermal gradient is small and a highly refined region where the gradient is large. The refined region is located at the inner diameter and varies from 0.25 inches to 1.0 inch depending on the depth of the hot zone of the particular stack. Figure 5 shows the finite element model of stack 7.

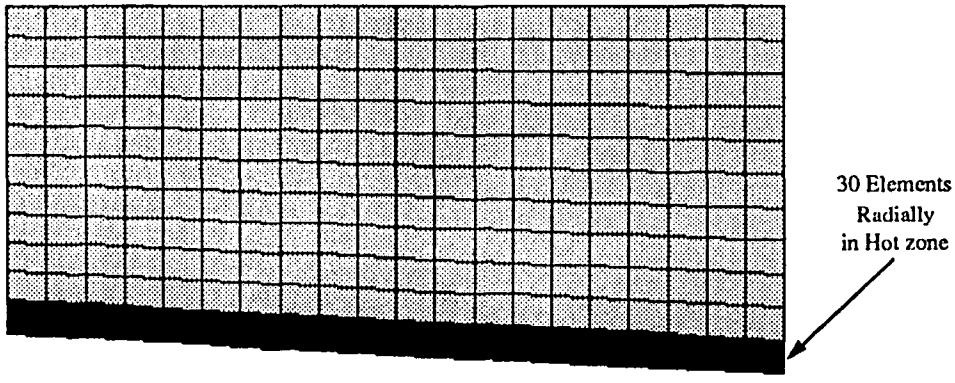


**Figure 5. Local Finite Element Model of Stack 7.**

## 7.3 Results

The only loads used to determine the deflections of the stacks were thermal gradients. The detailed analysis to determine the thermal gradients is in Appendix I. Figure 6 shows the stress and deflection results of the model of stack 7.

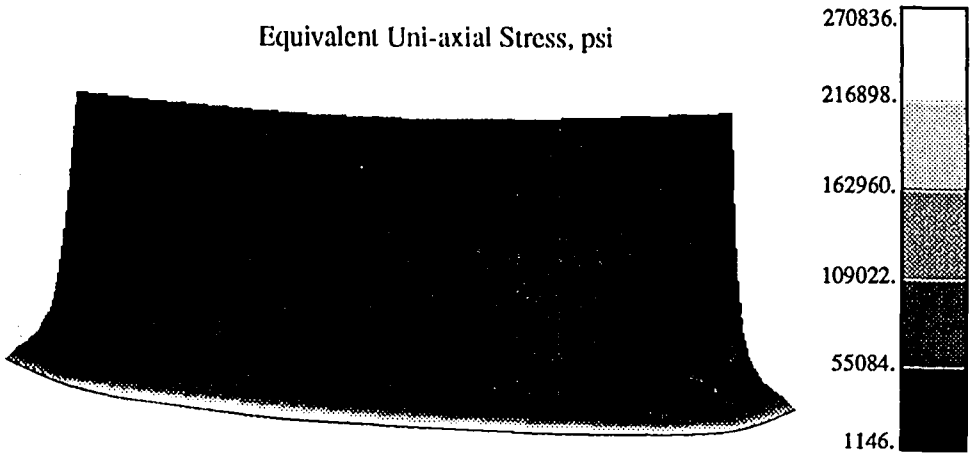


**Figure 6. Stress / Deformation Plot of Stack 7 under Thermal Loads.**

The results indicate that stacks 6, 7, 8, 10, 14, and 16 expand at the inner diameter relative to the room temperature state to .00617, .00426, .00400, .00867, .01232, and .01129 inches respectively. The remaining stacks used adjacent values ratioed by their respective lengths (assumed linear). These values were then compared to bulk temperature deflections and the local tolerancing criteria to obtain a tolerance layout.

## 8.0 Tolerance Layout

Figure 9 shows the variables and considerations used to determine the tolerance layout. The bulk temperature case used was the 4000. psi Hot-Min (worst case) condition.

**Table 7. Development of Tolerance Layout.**

| | Stack No. | | | | | | | | |
|---|---|---|---|---|---|---|---|---|---|
| **Variable** | **6** | **7** | **8** | **9** | **10** | **12** | **14** | **15** | **16** |
| 1. $\Delta T_{bulk}$ | -15 | -40 | -70 | -75 | -80 | -70 | -60 | -65 | -20 |
| 2. L | 5.75 | 5.75 | 5.15 | 5.15 | 8.7 | 5.3 | 7.87 | 8.38 | 15.5 |
| 3. $\Delta L_{bulk}$ | -.00078 | -.0021 | -.0032 | -.0035 | -.0063 | -.0033 | -.0042 | -.0049 | -.0028 |
| 4. $\Delta L_{ID}$ | .0062 | .0043 | .0040 | .0040 | .0087 | .0053 | .0123 | .0131 | .0113 |
| 5. $\Delta L_{ID} - \Delta L_{bulk}$ | .007 | .0064 | .0072 | .0075 | .0150 | .0086 | .0165 | .0180 | .0141 |
| 6. $(\Delta L_{ID} - \Delta L_{bulk})/3$ | .0023 | .0021 | .0024 | .0025 | .0050 | .0029 | .0055 | .0060 | .0047 |
| 7. Avail. Tolerance | .0044 | | .0049 | | .0079 | | .0115 | | .0047 |
| 8. Needed Tolerance | .0128 | | .0034 | | .0145 | | .0075 | | .009 |
| 9. Tolerance | .0084 | | -.0015 | | .0066 | | -.004 | | .0043 |
| 10. USE | .001<br>.002 | .007<br>.008 | | | | .007<br>.008 | .001<br>.002 | | .002<br>.003 |

The variables in Table 7 are defined below.

1. $\Delta T_{bulk}$ is bulk temperature difference between the platelet stacks and the housings under the 4000. psi Hot-Min case as describedin Table 4.
2. L is the length of the platelet stacks.
3. $\Delta L_{bulk}$ is the change in length between room temperature and the bulk temperature.
4. $\Delta L_{ID}$ is the change in length between room temperature and the maximum expansion at the inner diameter from the local FEM's of the stacks.
5. $\Delta L_{ID} - \Delta L_{bulk}$ is the additional deflection at the inner diameter as described in Figure 4.
6. $(\Delta L_{ID} - \Delta L_{bulk})/3$ is the amount available for tolerances as described in Figure 4.
7. The available tolerances summed over several stacks.
8. The over tolerance needed as determined by the bulk temperature analysis with zero flange gaps.
9. The difference between (8.) Needed Tolerance and (7.) Avail. Tolerance.
10. USE is the range of tolerance values in practical terms to accommodate (9.) Tolerance values.

The three main factors in Table 7 are; the bulk temperature state of the platelets (3.), the maximum deflection at the inner diameter from the local FEM's (4.), and the required tolerance determined from bulk temperature model with zero flange gaps(8.). From (3.) and (4.) above, the amount available for tolerances is determined and subtracted from the required tolerance which leaves the amount the stacks need to be oversized. Engineering judgement and practicality motivated the transition from the calculated values (9.) and the values that will actually be used (10.).The final tolerance values are graphically shown in Figure 7. The gaps between stacks 2, 3, and 4 and housing (-554) were chosen to insure that stack 5 bottomed out against housing (-554). The flange gap at station -16.0 was chosen to limit the stresses in housing (-553) due to preload and the high temperature stacks 1 and 2 can develope.

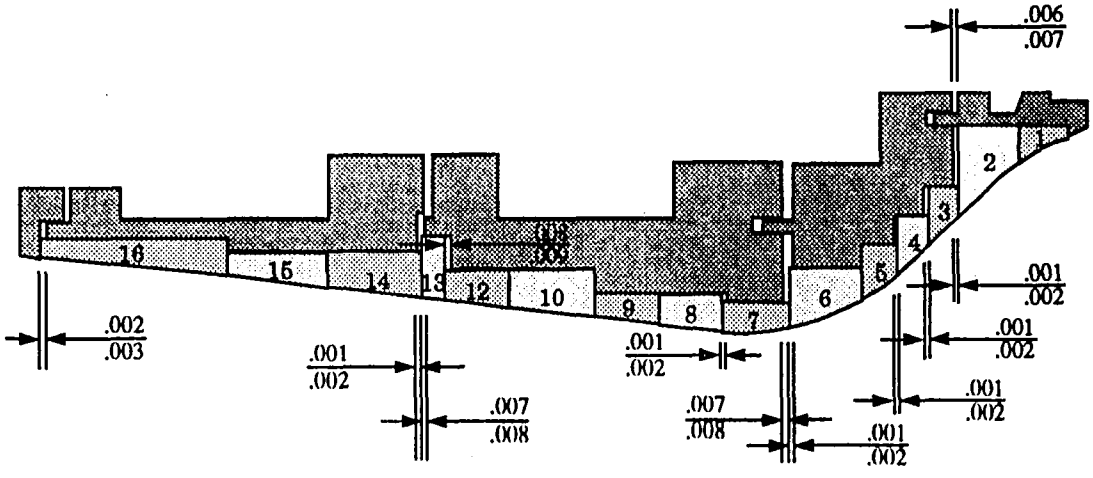


**Figure 7. Tolerance Layout.**

## 8.1 Results

The global model was run using the tolerance values in Figure 7. The upper bound of .010 inch flange gaps at stations 27.25 and -2.75 was used in the analysis. Figure 8 is a stress and deformation plot under the preload room temperature condition. It shows that the stresses are significantly reduced in stack 12 to an acceptable range. Therefore the structural criteria are met under the tolerance layout in Figure 7. The clearance between circuits will be evaluated in Section 9.

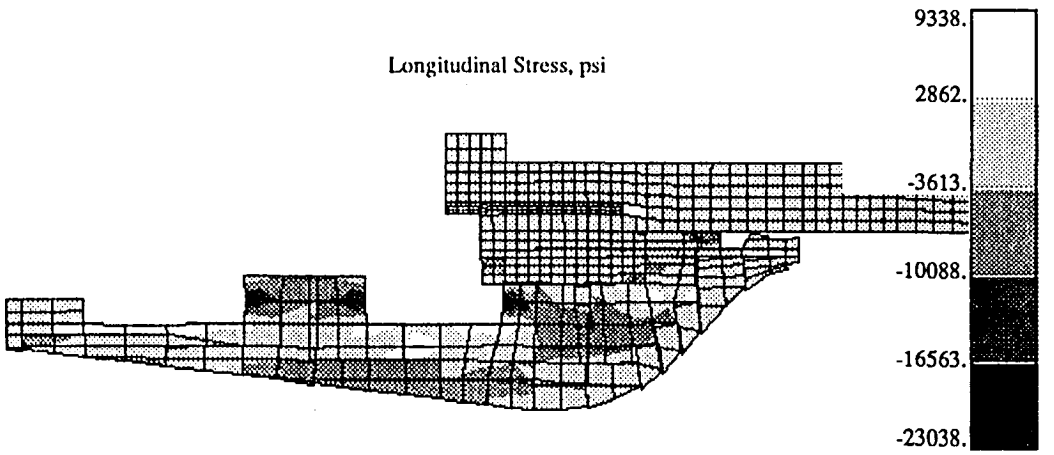


**Figure 8. Stress / Deformation Plot under Preload w/gaps = .010/.010**

The 700 psi cold condition was run to determine the maximum possible gapping between the platelet stacks. Figure 9 is a stress and deformation plot under the cold condition showing three gaps between the stacks. The actual location of the gaps will vary and the gap values only give a relative magnitude of the size of the gaps that may be distributed throughout the platelet stacks. The most realistic location for gaps to occur is at the throat. The most unrealistic location is in the contraction section.

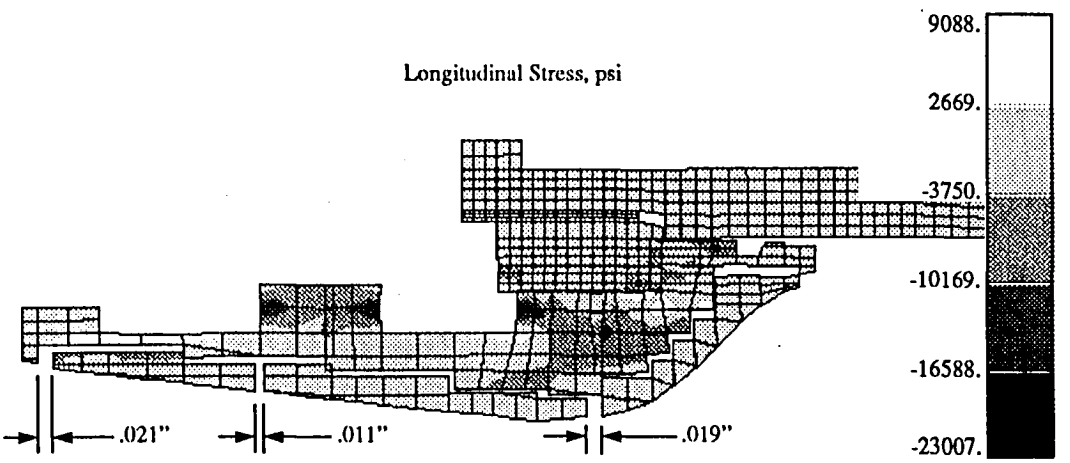


**Figure 9. Stress / Deformation Plot under 700 psi Cold Condition.**

# 9.0 Clearance Between Circuits

Table 8 shows the predicted clearances between the circuits under hot run conditions. The clearance is the gap between a platelet stack and the pressure shell at an interface between two circuits. These values were determined by considering the preload state and the local effects of stack heating.

**Table 8. Clearance Between Circuits.**

| Circuit | Clearance |
|---|---|
| 1 - 2 | .002 |
| 2 - 3 | .006 |
| 3 - 4 | .003 |
| 4 - 5 | .002 |
| 5 - 6 | .001 |
| 6 - 7 | .001 |
| 7 - 8 | .000 |

To evaluate the effect of the clearances on the performance of the circuits a mass flow model was developed. The details of the mass flow model are described in Appendix II.

## 9.1 Results from Mass Flow Model

Figure 10 shows the results of the mass flow model as described in Appendix II. It is a plot of the percent difference between a case with zero clearances between circuits and the clearances from Table 8, versus the circuit number. The highest percent difference is in circuit 6. This is the result of the high pressure from circuit 5 leaking into circuit 6. The 5% difference in circuit 6 meets the performance criteria of the nozzle.

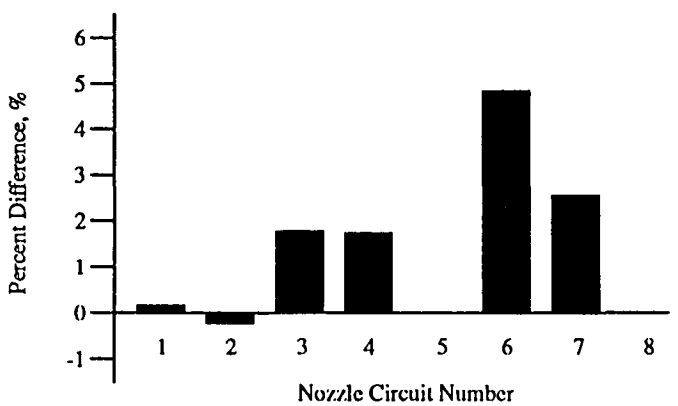


**Figure 10. Effects of Clearances Between Circuits.**

## 10.0 Bolt Preloads

The bolt torques are shown in Table 9. As a reference, the bolt stresses are given along with the percent of yield stress the bolts attain under the applied torque. In addition, the values used in the original design analysis are shown for comparison. The torques did increase from the original values but they are well within typical design torque values. Although these values are specified, the design philosophy is to ensure that all the flange joints pull up metal to metal. Therefore standard torquing methods are acceptable for all flange joints.

**Table 9. Bolt Torques.**

| | Station | | | |
|---|---|---|---|---|
| | 60.52 | 27.25 | -2.75 | -16.0 |
| Stress, ksi | 30.0 | 45.0 | 52.0 | 78.0 |
| % Yield | 23% | 35% | 40% | 60% |
| Torque, ft-lbs | 810 | 6020 | 5020 | 380 |
| **Original - for Comparison only** | | | | |
| Stress, ksi | 19.6 | 18.3 | 32.9 | 70.8 |
| % Yield | 15% | 14% | 25% | 55% |
| Torque, ft-lbs | 520 | 2440 | 3165 | 330 |

## 11.0 Assembly Procedure

The assembly procedure is described below. This procedure is based on performing the final full torque at station -2.75 since the other three stations load up only several stacks at a time while station -2.75 loads up all platelet stacks.

1. Install stacks 1 and 2 into housing -553.
2. Install stacks 5, 4, and 3 into housing -554.
3. Assemble housings -553 and -554 and torque station -16.0 to 380. ft-lbs.
4. Install stack 6 and assemble housings -553 and -554 into the combustor.
5. Assemble housings -554 and -555 and torque station -2.75 to 100. ft-lbs.
6. Install stacks 16, 15, and 14 into housing -556.
7. Assemble housings -555 and -556 and torque station -27.25 to 100. ft-lbs.
8. Torque station 60.52 to 810. ft-lbs.
9. Torque station 27.25 to 6020. ft-lbs.
10. Torque station -2.75 to 5020. ft-lbs.

## 12.0 Conclusions

An analysis has been performed to determine the tolerance layout between the platelets and the housing to meet the structural and performance criteria under a range of thermal, pressure, and bolt preload conditions. A finite element model of the nozzle was constructed to determine the global effects of the loads on the platelets, housings, and bolts. A tolerance layout was determined using the global model and the analysis revealed that high stresses occurred under hot and preload conditions. Under the hot cases only the under cooled conditions resulted in high stresses due to the high bulk temperatures of the stacks in circuits 1 and 8. Therefore 20% over cooling is required for circuits 1 and 8 or all circuits if desired. To lower the stresses under the preload condition, several models of the platelet stacks were constructed to take into account the local effects of stack heating and reduce the tolerance layout. A final tolerance layout was determined which meets the structural and performance criteria. In addition, a set of bolt torques are specified along with an assembly procedure.

## 13.0 Recomendations

- The tolerance layout shown in Figure 7, page 10, should be use when sizing the platelet stacks.
- The assembly procedure described in Section 11.0, page 13, should be followed using the bolt torques described in Section 10.0.
- Circuits 1 and 8 or all circuits if desired should be 20% over cooled relative to the original design values of cooling mass flow.

# Appendix I

# Thermal Analysis

## 1.0 Introduction

This analysis determines the temperature profiles of the transpiration cooled nozzle platelet stacks. The temperature profiles were used in local finite element models of the platelet stacks. This analysis took into account the temperature drop of the incoming coolant air. In addition, bulk temperatures were determined for the platelet stacks. These temperatures were used in the global finite element model of the nozzle.

The overall temperature drop of the incoming air was determined from two factors. The first is due to the expansion of the air in the bottle field as the pressure drops. This was modelled as a polytropic process with coefficients which have been determined experimentally. The second is due to the expansion of the air as it passes through the associated piping, valves, orifices and platelets. This was modelled as a Joule-Thomson process.

The temperature profiles of platelets at each end of each stack was determined from one-dimensional finite element models. Both the metal platelet and the coolant air was modelled. The mass weighted average temperature of each modelled platelet will then be determined. The bulk temperature of the platelet stack was determined by averaging the average temperatures of the two end platelets.

Temperatures profiles were calculated for three combustor pressures: 4000, 2000 and 700 psi. Both hot and cold runs were examined.

## 2.0 Cases Considered

The cases considered are shown in Section 4.0 Load Matrix, Table 2. The Hot cases are with methane burning in the combustor producing a high temperature gas to convect to the platelet stacks. The cases labeled Hot-Min have a nozzle cooling mass flow rate of 20 percent over design which gives lower platelet metal temperatures. Also considered in these cases is the lower coolant inlet temperature at the end of a run which would also give lower metal temperatures. The cases labeled Hot-Max have a nozzle cooling mass flow rate of 20 percent under design which gives higher metal temperatures. For the Cold cases, no combustion occurs and the platelet stack bulk temperatures are equal to the inlet coolant air temperature. A transient analysis showed this happens in less than two seconds.

# 3.0 Bottle Field Temperature Drop

The temperature drop of the bottle field was calculated using a polytropic relation along with measured data. The polytropic relation is;

$$pv^n = \text{Constant} \qquad \text{(EQ 1)}$$

or for an ideal gas this becomes;

$$Tp^{-\frac{(n-1)}{n}} = \text{Constant} \qquad \text{(EQ 2)}$$

Where 'p' is pressure, 'v' is the specific volume, 'T' is the temperature, and 'n' is the polytropic exponent. Note that the polytropic exponent is a function of the rate at which the mass flow leaves the bottle field. It has been assumed that for the 4000 psi case the mass flow is near the highest rate, for 700 psi the mass flow is near the lowest rate, and for the 2000 psi case the mass flow is linearly between the other two cases. The polytropic exponents for the 4000, 2000, and 700 psi combustor pressures are 1.13, 1.10, and 1.08 respectively as determined experimentally. The bottle field temperature drop for the three combustor pressures are calculated below.

## 3.1 4000 psi Case

$$p_i = 6000\text{psi} \quad p_f \geq 4500\text{psi} \quad n \approx 1.13 \quad T_i = 530°\text{R}$$

$$T_f = T_i\left(\frac{p_i}{p_f}\right)^{-\left(\frac{n-1}{n}\right)}$$

$$= 530\left(\frac{6000}{4500}\right)^{-\left(\frac{1.13-1}{1.13}\right)}$$

$$= 512.7$$

$$\Delta T \approx 20° \qquad \text{(EQ 3)}$$

Therefore, the expected temperature drop during a 4000 psi run is approximately 20 degrees.

### 3.2 2000 psi Case

$$p_i = 6000\text{psi} \qquad p_f \geq 2165\text{psi} \qquad n \approx 1.1 \qquad T_i = 530°\text{R}$$

$$T_f = T_i \left(\frac{p_i}{p_f}\right)^{\left(\frac{n-1}{n}\right)}$$

$$= 530 \left(\frac{6000}{2165}\right)^{-\left(\frac{1.1-1}{1.1}\right)}$$

$$= 483$$

$$\Delta T \approx 45°$$

(EQ 4)

Therefore, the expected temperature drop during a 2000 psi run is approximately 45 degrees.

### 3.3 700 psi Case

$$p_i = 6000\text{psi} \qquad p_f \geq 1000\text{psi} \qquad n \approx 1.08 \qquad T_i = 530°\text{R}$$

$$T_f = T_i \left(\frac{p_i}{p_f}\right)^{-\left(\frac{n-1}{n}\right)}$$

$$= 530 \left(\frac{6000}{1000}\right)^{-\left(\frac{1.08-1}{1.08}\right)}$$

$$= 464$$

$$\Delta T \approx 65°$$

(EQ 5)

Therefore, the expected temperature drop during a 700 psi run is approximately 65 degrees.

## 4.0 Joule - Thomson Effects

The temperature drop due to the pressure drop through the pipeline and valves between the bottle field and the platelet stacks was modelled as a Joule-Thomson process.

It was assumed that the Joule-Thomson process occurs between the bottle field pressure and the nozzle pressure at the inner diameter of the platelet stack. Table I-1 shows the temperature difference in degrees due to the Joule-Thomson effect for the three combustor pressures at the start of a run. At the interface between two stacks, the same temperature drop applies to both stacks at that location.

**Table I-1. Manifold Air Temperature Difference from Joule - Thomson Effects, $^{0}$R.**

| | Combustor Pressure, psi | | |
|---|---|---|---|
| Stack | 4000 | 2000 | 700 |
| 1 | -20 | -40 | -70 |
| 1-2 | -20 | -40 | -70 |
| 2-3 | -20 | -40 | -70 |
| 3-4 | -20 | -40 | -70 |
| 4-5 | -20 | -40 | -70 |
| 5-6 | -20 | -40 | -70 |
| 6-7 | -25 | -50 | -75 |
| 7-8 | -40 | -60 | -80 |
| 8-9 | -70 | -80 | -85 |
| 9-10 | -80 | -95 | -90 |
| 10-12 | -90 | -100 | -100 |
| 12-13 | -90 | -100 | -100 |
| 13-14 | -90 | -100 | -100 |
| 14-15 | -95 | -100 | -100 |
| 15-16 | -100 | -100 | -100 |
| 16 | -100 | -100 | -100 |

## 5.0 Coolant Inlet Temperatures

The coolant inlet temperature was determined based on the bottle field temperature and the Joule-Thomson effects. For each of the three combustor pressures, there were three cases considered; Hot-Max, Hot-Min, and Cold. For the Hot-Max case, temperature differences are those shown in Table I-1. These cases are considered as the 'start of a run' and therefore does not include any bottle field temperature drops. The inlet temperatures for the Hot-Min case used the 'end of a run' values of bottle field and Joule-Thomson effects. After tabulating the values for the 'end of run' condition it was determined that the values varied with the 'start of a run' values by +/- $10^{0}$. It was then decided to conservatively assume that the 'end of a run' was $10^{0}$ cooler than the 'start of a run' as tabulated in Table I-1. The inlet temperatures for the cold case were those used for the Hot-Min case.

# 6.0 Mass Flow and Heat Transfer Values

All mass flows, coolant and hot side heat transfer coefficients are taken from the original design calculations for the Transpiration Cooled Nozzle at 4000 psi combustor pressure. The mass flow rate was assumed to be linear with combustor pressure. The heat transfer coefficients were determined for the other combustor pressures by considering the Nusselt number as a function of Reynolds and Prandtl numbers of the form;

$$Nu = CRe^{0.8}Pr^{0.4} \quad \text{,which results in} \quad \frac{h}{h_{4000}} = \left(\frac{Re}{Re_{4000}}\frac{\mu_{4000}}{\mu}\right)^{0.8} .$$

# 7.0 Thermal Finite Element Model

To determine the temperature profiles through the transpiration cooled nozzle, one-dimensional thermal finite element models were created of a platelet set at each end of each platelet stack. A platelet set consists of a metering and a spacing platelet. The finite element models were processed using EAL (Ref. 1). The resulting temperature profiles were used to calculate bulk temperatures of each platelet stack.

## 7.1 Finite Element Model

A schematic of the finite element model is shown in Figure I-1. It consists of 82 nodes and 80 elements, half of which represent the metal and half of which represent the coolant air.

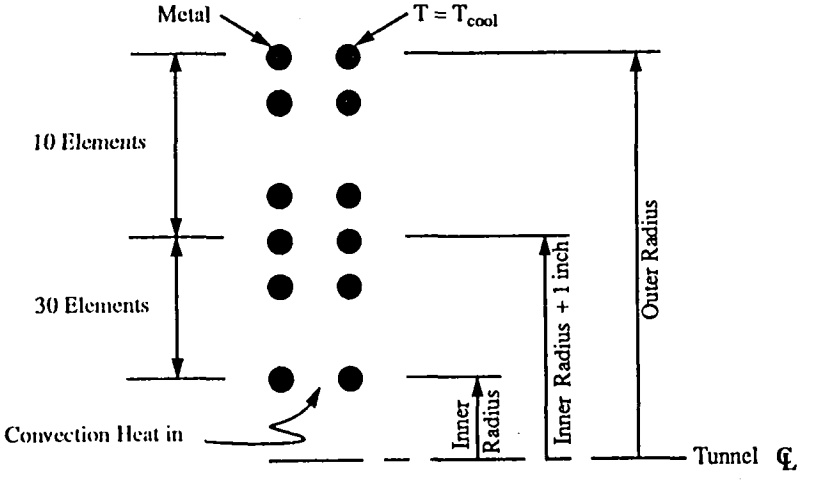


**Figure I-1. Thermal Finite Element Model.**

## 7.2 Assumptions

The combustor temperature is 4129 degrees R. A lower temperature will produce lower platelet stack temperatures unless the mass flow is reduced.

The initial bottle field pressure is 6000 psi. If the bottle field pressure is lower there will be less cooling by the Joule-Thomson effect and the platelet stacks will be at a higher temperature unless the cooling is increased.

Initial bulk temperatures of bottle field and nozzle housings are assumed to be the same. This should be true since both the nozzle and the bottle field are in buildings with similar climatic controls.

# 8.0 Results

The temperature profiles were determined for all platelet stacks and used to determine local deformations in selected platelet stacks and to determine bulk temperatures. As an example, Figure I-2 shows the temperature profile of stack 7 under the 4000 psi Hot-Min condition.

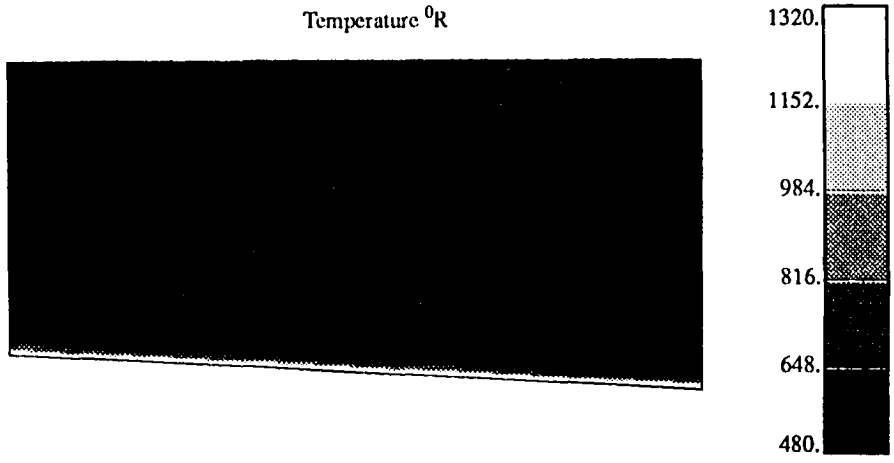


**Figure I-2. Temperature Profile for Stack 7 under 4000 psi Hot-Min Case.**

The bulk temperature for each platelet set and each end of a platelet stack is calculated by mass averaging. The bulk temperature for the stack is then taken as the mean of those two values. The bulk temperatures for the Hot-Max, Hot-Min, and cold cases for the three combustor pressures are shown in Section 4.2 Platelet Bulk Temperatures, Table 4.

# Appendix II

# Mass Flow Model

## 1.0 Introduction

This analysis determined the effect of circuit clearances and platelet gaps on the cooling flow rates to different circuits of the Transpiration Cooled Nozzle. The mass flow model was developed and run using ACSL (Ref. 3) dynamic simulation code. The results were used to evaluate gap and clearance defined by the global finite element model of the nozzle.

## 2.0 Method of Analysis

The Transpiration Cooled Nozzle was modeled using a lumped volume approach. The conservation equations of mass and energy were solved for each volume to determine temperature and pressure conditions. The conservation equations used in the analysis are;

$\dot{E} = c_p [\Sigma(\dot{m}_{in} T_{in}) - \Sigma(\dot{m}_{out} T_{out})]$ Volume Energy Derivative

$\dot{M} = \dot{m}_{in} - \dot{m}_{out}$ Volume Mass Derivative

$\dot{T} = (\dot{E}/c_v - \dot{M} T)/M$ Volume Temperature Derivative

$\dot{P} = (R/v)(M \dot{T} + T \dot{M})$ Volume Pressure Derivative

Where $c_p$ is the constant pressure specific heat coefficient, $c_v$ is the constant volume specific heat coefficient, v is the volume, and R is the real gas constant. The temperature and pressure derivatives were integrated to give volume states. Flow through the platelets was modeled using the quiet valve flow equations given in the Control Valve Handbook (Ref. 4). The equation is of the form;

$$\dot{m} = 4.84 \times 10^{-4} (P c_g / T^{1/2}) \sin[(59.64/c_1)(\Delta P/P)^{1/2}]$$

Where $c_g$ is the flow coefficient and $c_1$ is the recovery coefficient. For $\sin\theta$; where $\theta > \pi/2$, the flow is critical and the $\sin\theta$ is set to 1.0. Platelet $c_g$ was determined from original design data.

The orifice equation and critical flow table was taken from the Crane Manual (Ref. 5). Flow through clearances and gaps were modeled as Fanno flow. Loss coefficients and critical pressure drop tables were also taken from the Crane Manual. The equation for orifice flow is shown below.

$$\dot{m} = c_0 A Z P [(2 g/R T)(1 - P_{down}/P_{up})]^{1/2}$$

Where Z is the compressibility factor, $c_0$ is the orifice coefficient, A is the area, and g is the gravity term. The same general equation was used for clearance and gap flow with the coefficient, $c_0$, inclusive of friction and form loss. Values of $c_0$, Z, and the pressure ratio were adjusted for critical flow.

## 3.0 Mass Flow Model

Figure II-2 shows a schematic of the mass flow model. The nozzle receives air from two sources: the upstream and downstream air supply lines. The upstream line supplies air to circuits 1 through 4 and the downstream line supplies air to circuits 5 through 8. The clearances are modeled as valves between the eight manifold volumes. Each manifold volume supplies air to the platelet stacks in that circuit with the gaps modeled as circuits which starve the platelet stacks.

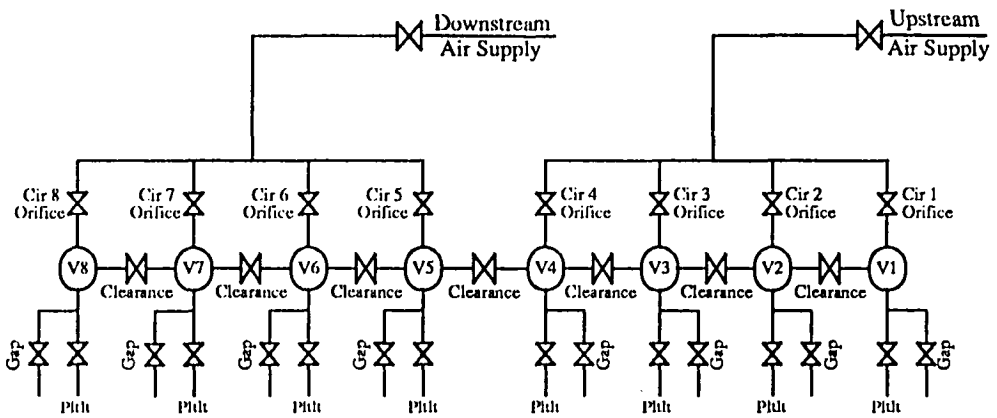


**Figure II-1. Schematic of Mass Flow Model.**

## 4.0 Results

Table II-1 shows the manifold pressures with no gaps or clearances and with the gaps and clearances from the structural analysis, Section 9.0 Clearance Between Circuits, Table 8. Also shown is the percent difference between the two.

**Table II-1. Manifold Pressures with and without Gaps and Clearances.**

| Circuit No. | No Clearance Pressure, psi | Clearance from Analysis Pressure, psi | %-Difference |
|---|---|---|---|
| 1 | 4345 | 4352 | .156 |
| 2 | 4395 | 4386 | -.211 |
| 3 | 4219 | 4294 | 1.766 |
| 4 | 3949 | 4016 | 1.725 |
| 5 | 3892 | 3891 | -.008 |
| 6 | 1252 | 1313 | 4.848 |
| 7 | 946 | 970 | 2.557 |
| 8 | 648 | 648 | 0.00 |

These results are described and graphically shown in Section 9.1 Results from Mass Flow Model.

# Appendix III

# Platelet Flutter Analysis

## 1.0 Introduction

During the first air test of the 8ft HTT Transpiration Cooled Nozzle, parts of the unbonded platelets were found in the test section. The failed segments consisted primarily of two typical pieces. As shown in Figure III-1, these parts are referred to as the 'dogleg' and the 'feeder tab'.

An analysis of the failed pieces was performed to assess possible failure mechanisms. During the evaluation of the unbonded platelets, it was determined that cold working of the platelet material would provide material strength characteristics similar to 347 SS in the full hard condition. Essentially, this would elevate the ultimate strength to 185 ksi.

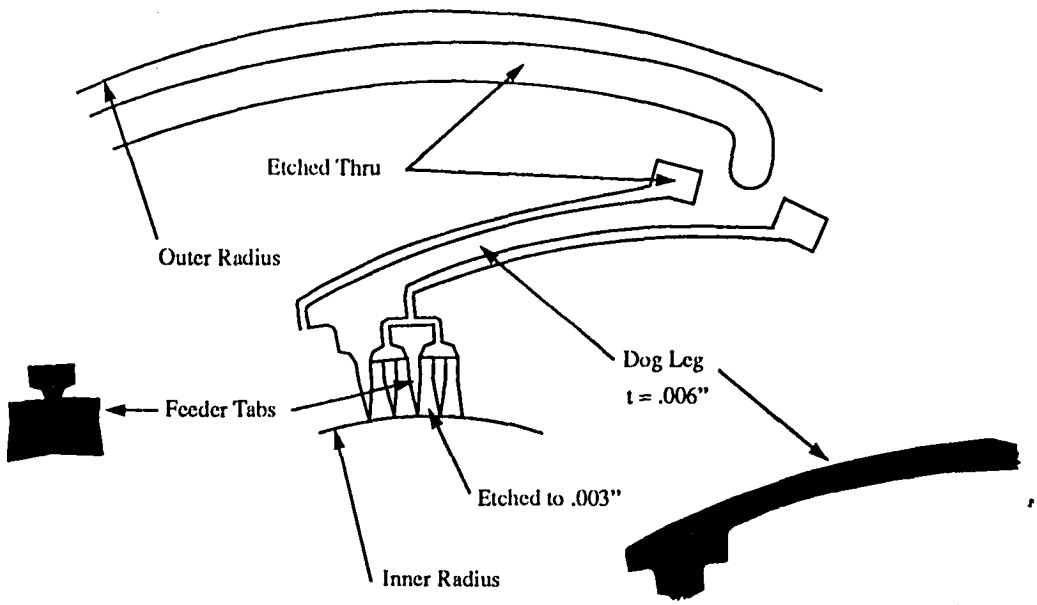


**Figure III-1. Platelet Configuration.**

## 2.0 Methods of Analysis

Using Fatigue reduction factors shown in Table III-1, a limit-cycle-motion analysis of the feeder tabs as a function of platelet gaps was performed. The limit cycle life in seconds was computed to estimate the time to failure for the feeder tabs given that the feeder tabs

were to under go large-amplitude vibration in a given gap between platelet stacks. The analysis of the feeder tabs was performed using a special purpose finite element code (Ref.-6) adapted for this particular case. The feeder tab was considered as a rectangular plate with two sides fixed and two sides free. Closed form techniques were used for the dog leg.

**Table III-1. Fatigue Reduction Factor for Unbonded Platelets.**

| Description | Value |
|---|---|
| Stress Concentration, kc | .500 |
| Surface Finish, ka | .650 |
| 99% Reliability, kr | .814 |
| Corrosion, kc | .500 |

## 3.0 Results

The results of the limit cycle analysis are presented in Table III-2. These results clearly indicate that as the gap opens, the feeder tabs are allowed to vibrate at larger amplitudes relative to the feeder tab thickness. In the gap, the feeder tabs are assumed to oscillate with peak-to-peak amplitudes equal to the gap opening. The estimated time to failure was found to fall of rapidly. Gaps of .005" to .008" were measured after the first air run. Also since the function of the nozzle is cooling, it is easily concluded that the actual gaps during the cold running of the nozzle were much larger than those values that were measured after the air test. Thus, it is postulated that this is a possible initial failure mechanism for the feeder tabs.

**Table III-2. Limit-Cycle Service Life Analysis Results.**

| Gap Size (inches) | Frequency (Hz) | Stress (ksi) | Service Life (seconds) |
|---|---|---|---|
| .004 | 4115. | 10.7 | Infinite |
| .005 | 4362. | 14.1 | 10820 |
| .006 | 4631. | 17.6 | 3588 |
| .007 | 5052. | 20.7 | 1532 |

Given that a feeder tab has failed and blown out of the nozzle, then a dogleg behaves as a cantilever section with a sharp notch at the support. When a pressure differential of 148 psi is applied across the long section of the dogleg, the resulting deflection is less than the width of the flow channel. However, the resulting stress is greater than the ultimate strength of the material in the full hard condition. This will result in the dog legs failing at the cantilever section; and with the feeder tabs blown out, the doglegs have enough open clearance in the flow passages to also be blown out.

Thus, the two mechanisms described above could result in a possible failure scenario for the unbonded platelets.

# References


1. Whetstone, W. D., EISI-EAL Engineering Analysis Language Reference Manual EISI-EAL System Level 312. Engineering Information Systems, Inc., August 1985.
2. Patran Division/PDA engineering, Patran Plus Users Manual Vol. 1 and 2, July 1988.
3. Mitchell & Gauthier Associates Inc., Advanced Continuous Simulation Language (ACSL), Level 10, October 1990.
4. Fisher Controls, Control Valve Handbook, Second Edition, Fisher Controls International, Inc., 1977
5. Crane Engineering Division, Flow of Fluids through Valves, Fittings, and Pipe, Crane Co., Technical Paper No. 410, 1981.
6. C. E. Chiang, C. Mei, and C. E. Gray, Jr., "Finite Element Large-Amplitude Free and Forced Vibrations of Rectangular Thin Composite Plates", Journal of Vibration and Acoustics, July 1991, Vol.113.

# REPORT DOCUMENTATION PAGE

*Form Approved*
*OMB No. 0704-0188*



| 1. AGENCY USE ONLY *(Leave blank)* | 2. REPORT DATE | 3. REPORT TYPE AND DATES COVERED |
|---|---|---|
| | February 1992 | Technical Memorandum |

**4. TITLE AND SUBTITLE**

8 ft HTT Transpiration Cooled Nozzle Thermal/Structural Analysis

**5. FUNDING NUMBERS**

WU 505-80-31-01

**6. AUTHOR(S)** Peyton B. Gregory, Jon E. Thompson, Dale A. Babcock, Carl E. Gray, Jr., Chris A. Mouring

**7. PERFORMING ORGANIZATION NAME(S) AND ADDRESS(ES)**
NASA Langley Research Center
Hampton, VA 23665-5225

**8. PERFORMING ORGANIZATION REPORT NUMBER**

**9. SPONSORING / MONITORING AGENCY NAME(S) AND ADDRESS(ES)**
National Aeronautics and Space Administration
Washington, DC 20546-0001

**10. SPONSORING / MONITORING AGENCY REPORT NUMBER**

NASA TM-104184

**11. SUPPLEMENTARY NOTES**

**12a. DISTRIBUTION / AVAILABILITY STATEMENT**

Unclassified - Unlimited
Subject Category - 39

**12b. DISTRIBUTION CODE**

**13. ABSTRACT** *(Maximum 200 words)*

The 8-foot High Temperature Tunnel (HTT) at NASA Langley Research Center is a combustion driven, high enthalpy blow down wind tunnel. In March, 1991, during check out of the transpiration cooled nozzle, pieces of platelets were found in the tunnel test section. It was determined that incorrect tolerancing between the platelets and the housing was the primary cause of the platelet failure. An analysis was performed to determine the tolerance layout between the platelets and the housing to meet the structural and performance criteria under a range of thermal, pressure and bolt preload conditions. Three recomendations resulted as a product of this analysis.

**14. SUBJECT TERMS**

Transpiration Cooled Nozzle
Structural Analysis
Thermal Analysis
Finite Element Analysis

**15. NUMBER OF PAGES**

32

**16. PRICE CODE**

A03

| 17. SECURITY CLASSIFICATION OF REPORT | 18. SECURITY CLASSIFICATION OF THIS PAGE | 19. SECURITY CLASSIFICATION OF ABSTRACT | 20. LIMITATION OF ABSTRACT |
|---|---|---|---|
| Unclassified | Unclassified | Unclassified | UL |

NSN 7540-01-280-5500

Standard Form 298 (Rev. 2-89)
Prescribed by ANSI Std. Z39-18
298-102